Scientific paper

Zinc(II) Thiosemicarbazone Complex As a Ligand Towards Some Transition Metal Ions: Synthesis, Spectroscopic and Antimicrobial Studies

Saied M. E. Khalil,[1,2]* Magdy Shebl[2] and Faizah S. Al-Gohani[1]

[1] *Chemistry Department, Faculty of Science, Taibah University, 30002 Al-Madena Al-Mounnawara, Saudi Arabia*

[2] *Chemistry Department, Faculty of Education, Ain Shams University, Roxy, Cairo, Egypt*

* *Corresponding author: E-mail: smekhalil@hotmail.com*

Received: 14-01-2010

Abstract

Heterobinuclear complexes have been synthesized by stepwise reactions using the mononuclear complex, $[Zn(Tsc)_2] \cdot H_2O$, as a complex ligand towards the metal ions, vanadyl(IV), manganese(II), iron(III), cobalt(II), nickel(II) and copper(II). The complex ligand was synthesized by the reaction of zinc acetate dihydrate with salicylaldehyde followed by the condensation with thiosemicarbazide. The structures of the complex ligand and the prepared complexes were elucidated by elemental analyses, IR, electronic, mass, ^{1}H and ^{13}C NMR spectra as well as molar conductivity and magnetic susceptibility measurements. All the complexes exhibited octahedral geometrical arrangements formulated as $[Zn(Tsc)_2VO(SO_4)(H_2O)]$, $[Zn(Tsc)_2MCl_2(H_2O)_2]$ (M = Mn, Fe and Co) and $[Zn(Tsc)_2Fe(ox)Cl2]$ except the nickel(II) and copper(II) complexes, $[Zn(Tsc)_2CuCl(H_2O)]$, $[Zn(Tsc)_2NiCl_2]$, which have square planar geometries. The complex ligand and some of its heterobinuclear complexes showed antibacterial activity against the sensitive organisms *Staphylococcus aureus* as Gram–positive bacteria, *Escherichia coli* as Gram–negative bacteria and antifungal activity against the fungi *Candida albicans* and *Aspergillus flavus*.

Keywords: Heterobinuclear complexes; mononuclear complexes; complex ligand; Thiosemicarbazones; ^{13}C NMR spectra; Antimicrobial activity

1. Introduction

Thiosemicarbazones and their metal complexes present a wide range of applications that stretch from their use in analytical chemistry, through pharmacology to nuclear medicine.[1–4] The presence of amide, imine and thione groups makes them potential polydentate ligands[5,6] and it is not surprising that numerous thiosemicarbazone complexes have been prepared and characterized.[7] In addition, in the last few years there has been a growing attention towards thiosemicarbazones related to their range of biological properties, specifically as antifungal, antiviral, antibacterial and anticancer agents.[8–18]

The search for new synthetic routes to multimetallic complexes is pertinent in coordination chemistry and crystal engineering.[19] Binuclear complexes particularly heterobinuclear systems[20,21] are of special interest due to their relevance to different branches on natural science, physics, chemistry and biology. Interest in polynuclear complexes is stimulated by the relevance of these compounds in molecular magnetism, material sciences, industrial catalysis, and bioinorganic chemistry, and they are ubiquitous in nature as active sites in a variety of metalloenzymes.[22–25] In the present work, we have synthesized the mononuclear complex, $[Zn(Tsc)_2] \cdot H_2O$, through the reaction of zinc acetate dihydrate with salicylaldehyde followed by the condensation with thiosemicarbazide. The use of this complex as a ligand towards vanadyl(IV), manganese(II), iron(III), cobalt(II), nickel(II) and copper(II) yielded a series of heterobinuclear complexes with different modes of bonding. However, mononuclear zinc(II) complex, $[Zn(Tsc)(H_2O)]$, was obtained from the reaction of the complex ligand with zinc(II) ion. The structures of the complex ligand and the prepared complexes were characterized by elemental analyses, IR, electronic, mass, ^{1}H and ^{13}C NMR spectra as well as molar conductivity and magnetic susceptibility measurements. The prepared compounds showed antibacterial activity against the sensitive organisms *Staphylococcus aureus* and *Escherichia coli* and antifungal activity against the fungi *Candida albicans* and *Aspergillus flavus*.

2. Experimental

2. 1. Materials

Manganese(II), iron(III), cobalt(II), nickel(II), copper(II) and zinc(II) were used as chloride salts and were Merck or BDH. Zinc(II) acetate, vanadyl(IV) sulphate, salicylaldehyde, thiosemicarbazide, oxalic acid, lithium hydroxide were BDH or Analar. Organic solvents (ethanol, absolute ethanol, methanol, diethylether, dimethylformamide (DMF) and dimethylsulfoxide (DMSO)) were reagent grade chemicals and were used without further purification.

2. 2. Measurements

Microanalyses of carbon, hydrogen, nitrogen, sulfur and chlorine were carried out on a Perkin Elmer 2400(USA) instrument at the Microanalytical Center, Cairo University, Giza, Egypt. FT-IR spectra were recorded on a Perkin-Elmer 598 spectrometer (4000–400 cm^{-1}) in KBr pellets. Mass spectra were recorded at 70 eV and 300 °C on a GC MS-QP 100 Ex 5988 mass spectrometer. Electronic spectra were recorded at room temperature on a Jasco model V-550 UV/Vis spectrophotometer as solutions in DMF. The ^1H and ^{13}C NMR spectra, as solutions in DMSO-d_6, were recorded on a Bruker WP 200 SY spectrometer at room temperature using TMS as an internal standard. Molar conductivities of 10^{-3} M solutions of the solid complexes in DMF were measured on the Corning conductivity meter NY 14831 model 441. Magnetic susceptibilities of the complexes were measured by the Gouy method at room temperature using a Johnson Matthey, Alfa Products, Model MKI magnetic susceptibility balance. The effective magnetic moments were calculated from the expression $\mu_{eff.} = 2.828 (\chi_M.T)^{1/2}$ B.M., where χ_M is the molar susceptibility corrected using Pascal's constants for the diamagnetism of all atoms in the compounds. Analyses of the metals were carried out using ICP Perkin Elmer Precisely Optical Emission Optima Spectrometer 2100 DV. Melting points of the complexes were determined using a Stuart melting point instrument. The antimicrobial activity was carried out at the Microanalytical Center, Cairo University, Giza, Egypt.

2. 3. Synthesis of the Organic Ligand, H_2L (1)

A mixture of salicylaldehyde, (2.3 mL, 21 mmol) and thiosemicarbazide (1.92 g, 21.0 mmol) in absolute ethanol was refluxed for 3 h. where a yellow precipitate was formed on hot, then allowed to cool slowly and collected by filtration, washed with ethanol then diethylether and finally air-dried. The yield was 86%, m.p. 230–232 °C.

2. 3. 1. Synthesis of Zinc(II) Complex of the H_2L ligand, [Zn(Tsc)OAc)] · ½H_2O (2)

An ethanolic solution (30 mL) of $Zn(OAc)_2 \cdot 2H_2O$ (1.13 g, 5.15 mmol) was added gradually to an ethanolic solution (40 mL) of the ligand (1.0 g, 5.12 mmol). The solution was refluxed for 2 h. and a dark yellow precipitate was formed. The precipitate was filtered off, washed with ethanol then diethylether and finally air-dried. The yield was 81%, m.p. >400 °C.

2. 3. 2. Synthesis of the Complex Ligand, $[Zn(Tsc)_2] \cdot H_2O$ (3)

An ethanolic solution of salicylaldehyde (5.15 mL, 49 mmol) was added gradually to an ethanolic solution (30 mL) of $Zn(OAc)_2 \cdot 2H_2O$ (5.4 g, 24.6 mmol) in molar ratio 2:1(sal:Zn^{2+}). The mixture was stirred for 3 h. then a solution of thiosemicarbazide (4.48 g, 49.2 mmol) in ethanol (20 mL) was added and the resulting mixture was refluxed for 4 h. where a yellow precipitate was formed. The precipitate was filtered off, washed with ethanol then diethylether ether and finally air-dried. The yield was 75%, m.p. >400 °C. Figure 1 represents the synthesis of the complex ligand (**3**) as compared to the organic ligand H_2L (**1**) and its Zn(II) complex (**2**).

2. 4. Synthesis of the Metal Complexes

Lithium hydroxide monohydrate, LiOH H_2O in methanol was added gradually with constant stirring to the complex ligand, $[Zn(Tsc)_2] \cdot H_2O$, in ethanol, in molar ratio 2:1 (LiOH: $[Zn(Tsc)_2] \cdot H_2O$). Metal chloride in ethanol was added gradually with constant stirring to the above mixture in molar ratio 1:1 (metal ion:$[Zn(Tsc)_2] \cdot H_2O$). The resulting mixture was refluxed for 3 h. where solid precipitates were formed, filtered off and washed several times with ethanol then diethylether and finally air-dried. In case of VO(IV) complex, least amount of water was added to ensure the complete dissolution of $VOSO_4 \cdot H_2O$. In case of cobalt(II) and zinc(II) complexes (**8 and 11**), the complexes were synthesized only by stirring. The complexes are insoluble in common organic solvents but they are partially soluble in DMF and/or DMSO.

The following detailed preparations are given as examples and the other complexes were obtained similarly.

2. 4. 1. Synthesis of the $[Zn(Tsc)_2NiCl_2]$, Complex (9)

Lithium hydroxide monohydrate, LiOH · H_2O (0.185 g, 4.4 mmol) in methanol (10 mL) was added gradually with constant stirring to the complex ligand,

$[Zn(Tsc)_2] \cdot H_2O$, (1.0 g, 2.12 mmol) in ethanol. Nickel(II) chloride hexahydrate, $NiCl_2 \cdot 6H_2O$ (0.524 g, 2.2 mmol) in ethanol (20 mL) was added gradually with constant stirring to the above mixture. The resulting mixture was refluxed for 3 h. A reddish-orange precipitate was formed, filtered off and washed several times with small amounts of ethanol then diethylether and finally air-dried. The yield was 74 %, m.p. >400 °C.

2. 4. 2. Synthesis of the $[Zn(Tsc)(H_2O)]_2$ Complex (11)

Lithium hydroxide monohydrate, $LiOH \cdot H_2O$ (0.142 g, 3.4 mmol) in methanol (10 mL) was added gradually with constant stirring to the complex ligand, $[Zn(Tsc)_2] \cdot H_2O$, (0.8 g, 1.7 mmol) in ethanol. Zinc(II) chloride, $ZnCl_2$ (0.23 g, 1.7 mmol) in ethanol (20 mL) was added gradually with constant stirring to the above mixture. The resulting mixture was stirred for 3 h. A pale yellow precipitate was formed, filtered off and washed several times with least amounts of ethanol then diethylether and finally air-dried. The yield was 85%, m.p. >400 °C.

2. 5. Antimicrobial Activity

The standardized disc–agar diffusion method[26] was followed to determine the activity of the synthesized compounds against the sensitive organisms *Staphylococcus aureus* as Gram–positive bacteria, *Escherichia coli* as Gram–negative bacteria and the fungi *Candida albicans* and *Aspergillus flavus*. Tetracycline was used as a standard reference in the case of bacteria while Amphotricine B was used as a standard antifungal reference.

The tested compounds were dissolved in dimethylsulfoxide [(DMSO) which has no inhibition activity] to get concentration of 2 mg/mL. The test was performed on medium potato dextrose agar (PDA) which contains infusion of 200 g potatoes, 6 g dextrose and 15 g agar.[27] Uniform size filter paper disks (3 disks per compound) were impregnated by equal volume (10 μL) from the specific concentration of dissolved test compounds and carefully placed on incubated agar surface. After incubation for 36 h at 27 °C in the case of bacteria and for 48 h at 24 °C in the case of fungi, inhibition of the organisms which evidenced by clear zone surround each disk was measured and used to calculate mean of inhibition zones.

3. Results and Discussion

3. 1. Characterization of the Complex Ligand, $[Zn(Tsc)_2] \cdot H_2O$

The complex ligand, $[Zn(Tsc)_2] \cdot H_2O$, was prepared by the reaction of zinc(II) acetate with salicylaldehyde followed by the condensation with thiosemicarbazide. For comparison, zinc(II) complex of the organic H_2L ligand, which was formed by the condensation of salicylaldehyde with thiosemicarbazide, was synthesized and characterized. The analytical and spectroscopic methods showed that the complex ligand is completely different than the zinc(II) complex of the organic ligand.

The structure of the complex ligand was elucidated by elemental analyses, IR, electronic, ^1H and ^{13}C NMR spectra and the obtained data were compared with those for the oganic ligand, H_2L, and its Zn(II) complex **2**. The elemental analyses (Table 1) showed that the molecular formula for the complex ligand is $[Zn(Tsc)_2] \cdot H_2O$ while the organic ligand H_2L reacted with zinc(II) acetate dihydrate (either in 1:1 or 1:2 molar ratio) yielding $[Zn(Tsc)OAc)] \cdot ½H_2O$.

The IR spectrum of the H_2L ligand (Table 2) showed two strong bands at 3442 and 3319 cm^{-1} which may be assigned to ν_{as} and ν_s of the amino group, respectively. Also, the medium band observed at 3173 cm^{-1} may be assigned to ν(NH). The band observed at 2808 cm^{-1} may be assigned to the hydrogen bonded phenolic OH group, ν(OH). Finally, the strong bands at 1614, 1266 and 829 cm^{-1} may be attributed to ν(C=N), ν(C–O) phenolic and ν(C=S), respectively.

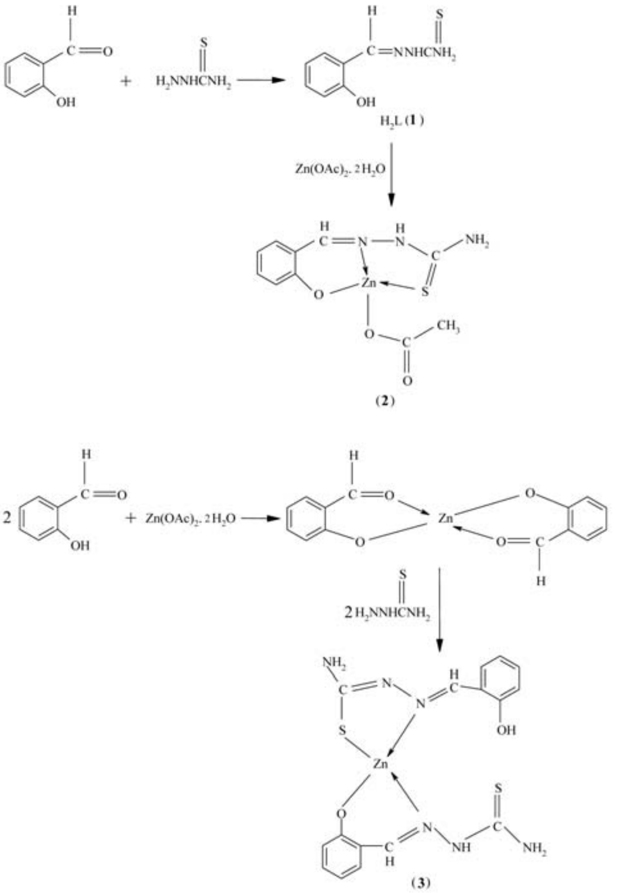

Figure 1. Synthesis of the complex ligand (**3**) as compared to the organic ligand H_2L(**1**) and its Zn(II) complex (**2**).

Table 1. Analytical and physical data of the complex ligand and its heterobinuclear complexes

No.	Reactions*	Complexes M. F. [F. Wt]	Color	Yield (%)	Elemental Analysis, % Found/(Calc.)						
					C	H	N	S	Cl	Zn	M
1	Salicylaldehyde + thiosemicarbazide (1:1)	H_2L $C_8H_9N_3OS$ [195.2]	Yellow	86	49.5 (49.2)	4.5 (4.6)	21.7 (21.5)	16.5 (16.4)	–	–	–
2	H_2L + $Zn(OAc)_2 \cdot 2H_2O$ (1:1 or 2:1)	$[Zn(HL)OAc)] \cdot ½H_2O$ $C_{10}H_{12}N_3O_{3.5}SZn$ [327.7]	Dark yellow	81	36.3 (36.7)	3.4 (3.7)	12.9 (12.8)	10.1 (9.8)	–	20.2 (19.9)	–
3	Salicylaldehyde + $Zn(OAc)_2 \cdot 2H_2O$ + thiosemicarbazide (2:1:2)	$[Zn(Tsc)_2] \cdot H_2O$ $C_{16}H_{18}N_6O_3S_2Zn$ [471.9]	Light yellow	75	40.4 (40.7)	4.0 (3.8)	17.5 (17.8)	14.0 (13.6)	–	14.0 (13.9)	–
4	$[Zn(Tsc)_2] \cdot H_2O$ + $LiOH \cdot H_2O$ + $VOSO_4 \cdot H_2O$	$[Zn(Tsc)_2VO(SO_4)(H_2O)]$ $C_{16}H_{18}N_6O_8S_3ZnV$ [634.9]	Green	82	30.7 (30.3)	3.1 (2.9)	12.9 (13.2)	14.8 (15.2)	–	9.9 (10.3)	7.8 (8.0)
5	$[Zn(Tsc)_2] \cdot H_2O$ + $LiOH \cdot H_2O$ + $MnCl_2 \cdot 4H_2O$	$[Zn(Tsc)_2MnCl_2(H_2O)_2]$ $C_{16}H_{20}N_6O_4S_2Cl_2ZnMn$ [615.7]	Brown	62	30.9 (31.2)	3.5 (3.3)	13.7 (13.6)	10.1 (10.4)	11.7 (11.5)	10.1 (10.6)	8.6 (8.9)
6	$[Zn(Tsc)_2] \cdot H_2O$ + $LiOH \cdot H_2O$ + $FeCl_3 \cdot 6H_2O$	$[Zn(Tsc)_2FeCl_2(H_2O)_2]$ $C_{16}H_{19}N_6O_4S_2Cl_2ZnFe$ [615.6]	Deep brown	89	31.4 (31.2)	3.3 (3.1)	13.3 (13.7)	10.7 (10.4)	11.4 (11.5)	10.4 (10.6)	8.9 (9.1)
7	$[Zn(Tsc)_2] \cdot H_2O$ + $LiOH \cdot H_2O$ + $FeCl_3 \cdot 6H_2O$ + oxalic acid (ox)	$[Zn(Tsc)_2Fe(ox)Cl_2]$ $C_{18}H_{17}N_6O_6S_2Cl_2ZnFe$ [669.6]	Reddish brown	89	32.1 (32.3)	2.6 (2.6)	12.4 (12.6)	9.7 (9.6)	10.1 (10.6)	10.1 (9.8)	8.3 (8.3)
8	$[Zn(Tsc)_2] \cdot H_2O$ + $LiOH \cdot H_2O$ + $CoCl_2 \cdot 6H_2O$	$[Zn(Tsc)_2CoCl_2(H_2O)_2]$ $C_{16}H_{20}N_6O_4S_2Cl_2ZnCo$ [619.7]	Brown	69	30.8 (31.0)	3.3 (3.3)	13.8 (13.6)	10.4 (10.3)	11.3 (11.4)	10.5 (10.5)	9.3 (9.5)
9	$[Zn(Tsc)_2] \cdot H_2O$ + $LiOH \cdot H_2O$ + $NiCl_2 \cdot 6H_2O$	$[Zn(Tsc)_2NiCl_2]$ $C_{16}H_{16}N_6O_2S_2Cl_2ZnNi$ [583.5]	Reddish orange	74	33.0 (32.9)	2.3 (2.8)	14.2 (14.4)	10.7 (11.0)	12.0 (12.2)	11.5 (11.2)	10.3 (10.1)
10	$[Zn(Tsc)_2] \cdot H_2O$ + $LiOH \cdot H_2O$ + $CuCl_2 \cdot 2H_2O$	$[Zn(Tsc)_2CuCl(H_2O)]$ $C_{16}H_{17}N_6O_3S_2ClZnCu$ [569.8]	Green	83	33.6 (33.7)	3.1 (3.0)	14.5 (14.7)	11.4 (11.3)	6.5 (6.2)	11.3 (11.5)	11.1 (11.2)
11	$[Zn(Tsc)_2] \cdot H_2O$ + $LiOH \cdot H_2O$ + $ZnCl_2$	$[Zn(Tsc)(H_2O)]$ $C_8H_9N_3O_2SZn$ [276.6]	Pale yellow	85	34.7 (34.7)	3.1 (3.3)	15.6 (15.2)	12.0 (11.6)	–	23.2 (23.6)	–

* All complexes are prepared either by stirring or reflux where the same complexes are obtained except complexes **8** and **11** which are obtained only by stirring.

Table 2. Characteristic IR spectral data (cm^{-1})[a] of the complex ligand and its complexes and their assignments

No.	Complexes	IR Spectra (cm^{-1})							
		$\nu_{as}(NH_2)$	$\nu_s(NH_2)$	ν(NH)	ν(C=N)	ν(C–O) phenolic	ν(N–N)	ν(C=S)	Other bands
1	H_2L	3442 s	3319 s	3173 m	1614 vs	1266 s	1060 m	1201 m, 829 s	
2	$[Zn(Tsc)OAc)]\cdot½H_2O$	3454 m	3317 s	3166 m	1597 s	1278 m	1046 m	1200 s, 801 s	1548 m, 1433 m; ν(CH_3COO^-) (monodentate)
3	$[Zn(Tsc)_2]\cdot H_2O$	3424 s	3313 m	3128 s	1605 s	1282 m	1062 m	1204 m, 805 s	1654 m; δOH (H_2O)
4	$[Zn(Tsc)_2VO(SO_4)(H_2O)]$	3424 sh	3313 s	3166 s	1604 vs	1284 s	1045 s	1207 m, 806 vs	1145 s, br 1126 s, br, 732 w; ν(SO_4^{2-}) (bidentate), 957; ν(V=O)
5	$[Zn(Tsc)_2MnCl_2(H_2O)_2]$	3450 m	3324 m	3159 m, br	1595 vs	1278 s	1034 m	1202 s, 801 s	3599 m, br, 3496 m, br; νOH (H_2O)
6	$[Zn(Tsc)_2FeCl_2(H_2O)_2]$	3421 vs, br	3301 s, br	3182 m, br	1600 vs	1296 m	1033 m	1207 m, 817 m	
7	$[Zn(Tsc)_2Fe(ox)Cl_2]$	3398 vs	3271 m	3159 m	1600 vs	1303 m	1033 m	1211 s, 821 vs	1666 vs; ν(oxalate) (bidentate)
8	$[Zn(Tsc)_2CoCl_2(H_2O)_2]$	3455 s, br	3346 s, br	3172 s, br	1599 s	1288 m	1038 m	1204 s, 812 m	3560 sh; νOH (H_2O)
9	$[Zn(Tsc)_2NiCl_2]$	3470 s, br	3314 s, br	3168 m	1604 s	1280 m	1038 m	1208 s, 808 s	
10	$[Zn(Tsc)_2CuCl(H_2O)]$	3447 s, br	3286 m	3145 m	1598 s	1277 s	1045 m	1210 s, 808 s	1634 m; δOH (H_2O), 3580 sh; νOH (H_2O)
11	$[Zn(Tsc)(H_2O)]$	3449 s	3310 m	3162 m	1595 s	1276 vs	1045 m	1198 s, 800 s	1623 s; ν(C=N), 3491; νOH (H_2O)

[a] s, strong; sh, shoulder; m, medium; w, weak; vs, very strong; br, broad; ν, stretching; δ, bending.

In the IR spectrum of the Zn(II) complex of H_2L ligand, the bands assigned to ν(C=N) and ν(C=S) were shifted to lower wave number, indicating the participation of these groups in chelation.[28,29] Also, the appearance of new bands at 1548 and 1433 cm^{-1} may be due to $\nu_{as}(COO^-)$ and $\nu_s(COO^-)$, respectively, of the CH_3COO^- group. The separation of the two bands, $\Delta\nu = (\nu_{as}-\nu_s)$ = 115 cm^{-1}, is comparable to the values cited for the monodentate character of the acetate group.[30] On the basis of the above interpretation, it was concluded that the ligand acted as a tridentate ligand through the azomethine nitrogen, thionic sulphur and phenolic oxygen. The complex ligand showed bands characteristic for $\nu_{as}(NH_2)$, $\nu_s(NH_2)$, ν(NH), ν(C=N) and ν(C=S) groups at nearly the same positions as H_2L ligand.

The electronic spectra of the H_2L ligand, its Zn(II) complex and the complex ligand in DMF (Table 3) showed three bands in the ranges 430–390, 350–310 and 270–256 nm. The higher energy band is assigned to π–π* transitions of the azomethine linkage and the aromatic benzene ring. The medium energy band is assigned to *n*–π* transitions while the lower energy band is attributed to charge transfer (CT) transitions within the molecule.

^1H and ^{13}C NMR spectral data (δ ppm) of the H_2L ligand, its Zn(II) complex and the complex ligand relative to TMS (0 ppm) in DMSO-d_6, Table 4, lend further sup-

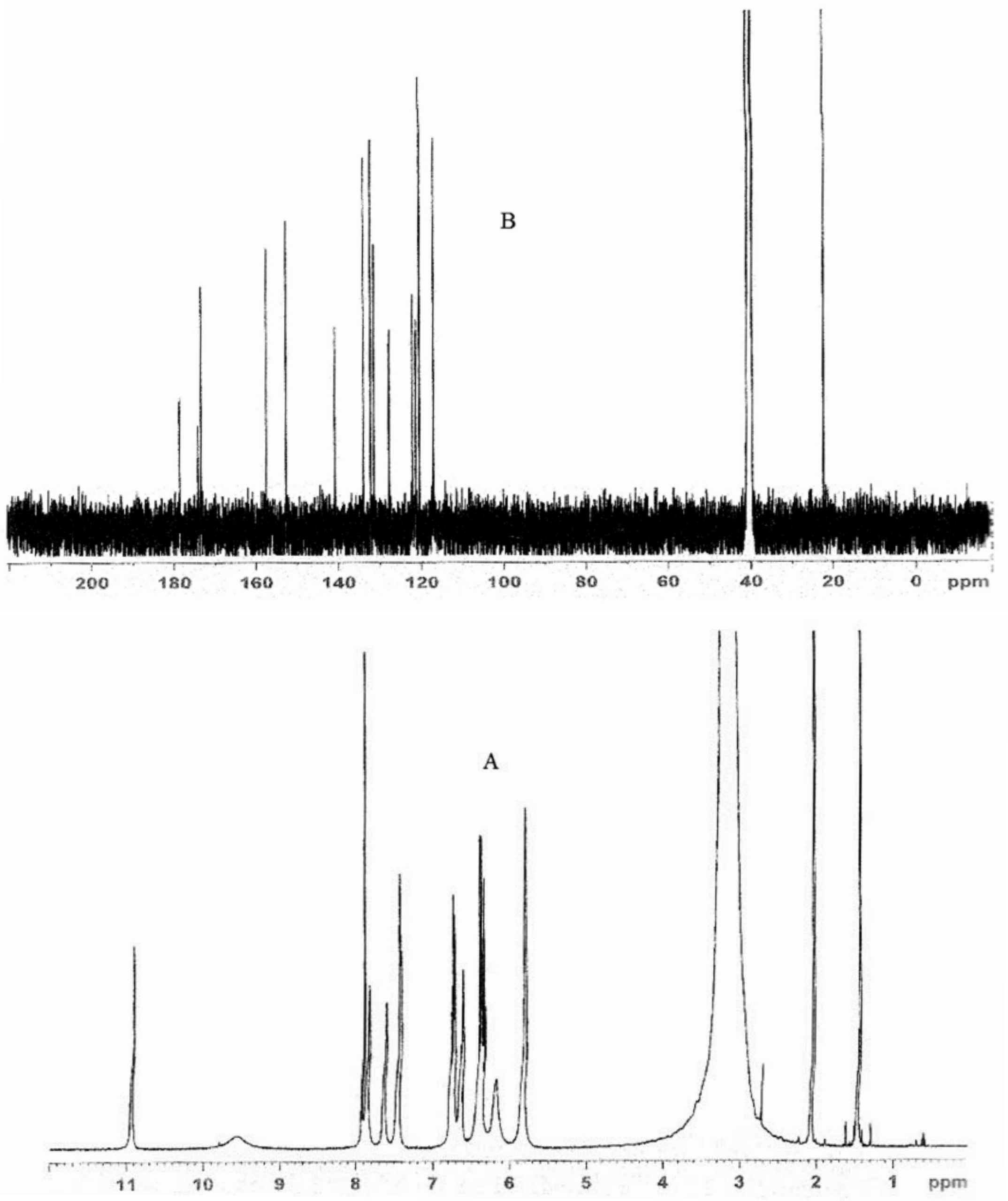

Figure 2. (A) ^1H and (B) ^{13}C NMR spectra of the complex ligand (**3**).

port of the suggested structures of them. In case of Zn(II) complex of H_2L ligand, $[Zn(HL)OAc)] \cdot ½H_2O$, the signal due to the phenolic OH proton was disappeared, indicating the deprotonation of this group upon complexation. The signal due NH group was shifted to 7.7 ppm however, the signal due to NH_2 group remained intact. Also, the new singal observed at 1.85 ppm may be due to the coordinated aectate group. This is supported by the ^{13}C NMR spectrum of the complex where new signals were obseved at δ = 173.5 and 22.5 ppm which may be assigned to the C=O and CH_3 groups of the acetate ion, respectively. Also, the signal due to the azomethine group was shifted downfield from 140.1 to 151.7 ppm, indicating that the Zn–N bond is more strong than Zn–O or Zn–S bonds.[31] The ^1H NMR spectrum of the complex ligand, $[Zn(Tsc)_2] \cdot H_2O$, (Figure 2) showed signals that support its suggested structure. One signal is observed for the phenolic OH proton at 10.9 ppm. In the ^{13}C NMR spectrum of the complex ligand (Figure 2), two signals were observed for each group (C=S, C–O and C=N groups), indicating the inequivalent coordination towards the Zn(II) ion. The mass spectrum of the complex ligand (Figure 3) showed the molecular ion peak at m/z 453, which compares well with the calculated formula weight of the anhydrous complex ligand, $[Zn(Tsc)_2]$, (F. Wt. 453.9).

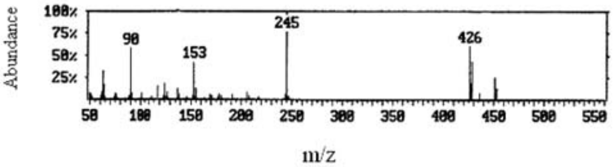

Figure 3. Mass spectrum of the complex ligand, $[Zn(Tsc)_2] \cdot H_2O$.

3. 2. Characterization of the Heterobinuclear Complexes

All of the prepared complexes were found to be stable at room temperature, non-hygroscopic and insoluble in water and most common organic solvents. The melting points of the complexes were found to be above 400 °C. The analytical and physical data for the complex ligand and its heterobinuclear complexes are listed in Table 1. The elemental analyses of the complexes agreed well with the proposed formulas.

3. 2. 1. IR Spectra

The IR spectral data are listed in Table 2. Comparison of the IR spectra of the complexes with that of the complex ligand revealed that the complexes showed band

Table 3. Electronic spectra, magnetic moments and molar conductivity data of the complex ligand and its complexes

No.	Complexes	Electronic spectral bands (nm)[a]	$\mu_{eff.}$ B.M.	Conductance[a] $Ohm^{-1}\ cm^2\ mol^{-1}$
1	H_2L	390 sh, 350, 256	–	–
2	$[Zn(Tsc)OAc)] \cdot ½H_2O$	410, 320, 270	Diam.	10
3	$[Zn(Tsc)_2] \cdot H_2O$	430, 310, 265	Diam.	9
4	$[Zn(Tsc)_2VO(SO_4)(H_2O)]$	610, 440	1.61	19
5	$[Zn(Tsc)_2MnCl_2(H_2O)_2]$	510	5.2	15
6	$[Zn(Tsc)_2FeCl_2(H_2O)_2]$	610, 510 sh, 450 sh	5.7	45
7	$[Zn(Tsc)_2Fe(ox)Cl_2]$	650, 530	5.8	22
8	$[Zn(Tsc)_2CoCl_2(H_2O)_2]$	520, 430 sh	5.0	23
9	$[Zn(Tsc)_2NiCl_2]$	565, 500	Diam.	10
10	$[Zn(Tsc)_2CuCl(H_2O)]$	580, 490	1.68	18
11	$[Zn(Tsc)(H_2O)]$	440	Diam.	8

[a] Solutions in DMF (10^{-3} M).

Table 4. ^1H and ^{13}C NMR spectral data[a] of the complex ligand and its diamagnetic complexes

	^1H assignments					^{13}C assignments				
Complexes	**OH**	**NH**	**HC=N**	**NH_2**	**CH_3**	**C=S**	**C–O phenolic**	**C=N**	**C=O**	**CH_3**
H_2L (**1**)	11.39 (b)	9.8 (b)	8.6	8.39	–	177.7	156.5	140.1	–	–
$[Zn(Tsc)OAc)] \cdot ½H_2O$ (**2**)	–	7.7 (b)	8.9	8.33	1.85	175.5	159.8	151.7	173.5	22.5
$[Zn(Tsc)_2] \cdot H_2O$ (**3**)	10.9	9.6	7.8, 7.9	7.4	–	178.6, 174.2	157.5, 152.7	140.9, 134.1	–	–
$[Zn(Tsc)_2NiCl_2]$ (**9**)	10.7	9.5	7.8, 7.9	7.35	–	176.6, 174.8	155.5, 151.5	138.2, 131.2	–	–
$[Zn(Tsc)(H_2O)]$ (**11**)	–	–	7.8	6.8	–	174.3	164.1	152.6	–	–

[a] b: broad

in the range 3599–3491 cm^{-1} assignable to $\nu(OH)$ of the coordinated or uncoordinated water molecules associated with the complexes which are confirmed by elemental analyses. Also, $\delta OH(H_2O)$ band is observed in the range 1654–1634. Also, the band at 1605 cm^{-1} assigned to $\nu(C=N)$ in the complex ligand was shifted to lower wave number in all of the complexes, indicating the participation of the azomethine nitrogen in chelation.[32–34] In complex **4**, the bands observed at 1145, 1126 and 732 cm^{-1} indicated the chelating bidentate SO_4^{2-} group.[35] Also, the characteristic band of the $\nu(V=O)$ is observed at 957 cm^{-1}.[36,37] In complexes **6** and **7**, the bands due to $\nu(NH_2)$ were shifted to lower wave number, indicating the participation of the amino group in chelation.[38] This is consistent with the fact that Fe^{3+} ion is a hard acid that prefers the NH_2 group (hard base) more than C=S group (soft base). In complex **7**, the new band observed at 1666 cm^{-1} may be due to the presence of the bidentate oxalate ion. This relatively higher value may indicate that one of the oxygen atoms of the oxalate group coordinates to the metal ion.[39]

3. 2. 2. Conductivity Measurements

The molar conductance values of the complexes in DMF (10^{-3} M solutions) were measured at room temperature and the results are listed in Table 3. The values show that all complexes have non-electrolytic nature. In case of complexes **6, 7** and **8**, the relatively high values of the molar conductance data may be due to the replacement of the coordinated chloride ions by solvent molecules, a phenomenon usually encountered in complexes containing chloride ions.[40]

3. 2. 3. Electronic Spectra and Magnetic Measurements

3. 2. 3. 1. The VO(IV) Complex

The VO(IV) complex, $[Zn(Tsc)_2VO(SO_4)(H_2O)]$ (Figure 4), was obtained from the reaction of the complex ligand with $VOSO_4 \cdot H_2O$. The electronic spectrum of the complex showed two bands at 610 and 440 nm. The first band is due to d-d transition and is consistent with the octahedral geometry[41] while the second band is due to charge transfer. The IR spectrum of the complex showed the coordination of the sulphate group as a bidentate ligand. The octahedral geometry is completed by a water molecule. The magnetic moment of the complex is 1.61 B.M. which is expected for d^1-system.

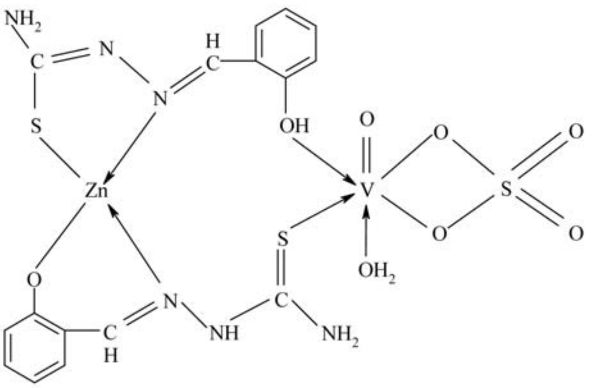

Figure 4. The proposed structure of the VO(IV) complex (**4**).

3. 2. 3. 2. The Mn(II) Complex

The reaction of $MnCl_2 \cdot 4H_2O$ with the complex ligand yielded the heterobinuclear complex, $[Zn(Tsc)_2MnCl_2(H_2O)_2]$, (Figure 5). The electronic spectrum of the obtained complex showed a band at 510 nm corresponding to the $^6A_{1g} \rightarrow {}^4T_{1g}$ transition which is consistent with the octahedral geometry of the complex.[42] The effective magnetic moment of the complex is 5.8 B.M. which falls in the range expected for octahedral manganese(II) complexes.[43,44]

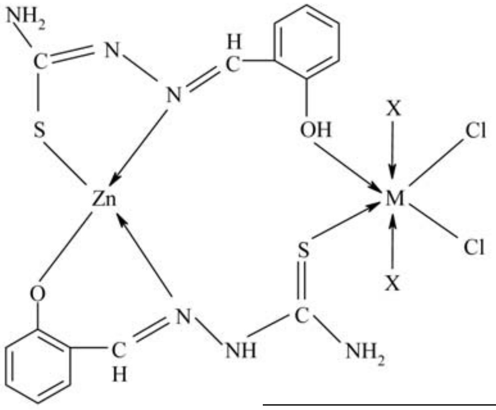

M	X	Complex
Mn	H_2O	**5**
Co	H_2O	**8**
Ni	nil	**9**

Figure 5. Proposed structures of the Mn(II), Co(II) and Ni(II) complexes.

3. 2. 3. 3. Fe(III) Complexes

The reaction of $FeCl_3 \cdot 6H_2O$ with the complex ligand yielded the heterobinuclear complex (**6**), $[Zn(Tsc)_2FeCl_2(H_2O)_2]$. Also, the reaction was carried out in the presence of oxalic acid, as a secondary ligand, giving the complex (**7**), $[Zn(Tsc)_2Fe(ox)Cl_2]$. The electronic spectra of the Fe(III) complexes (**6** and **7**) showed two absorption bands in each, the former complex (**6**) were at 610 and 510 nm and the latter complex (**7**) were at 650 and 530 nm. These bands are due to d-d transitions in an octahedral geometry.[45] The values of the magnetic moment of the iron(III) complexes (**6** and **7**) are 5.7 and 5.8 B.M., respectively which is consistent with the presence of five unpaired electrons in the Fe(III) ion in an octahedral geometry.[46] Based on the above interpretation, as well as the IR spectral data, tentative structures of these complexes are shown in Figures 6 and 7.

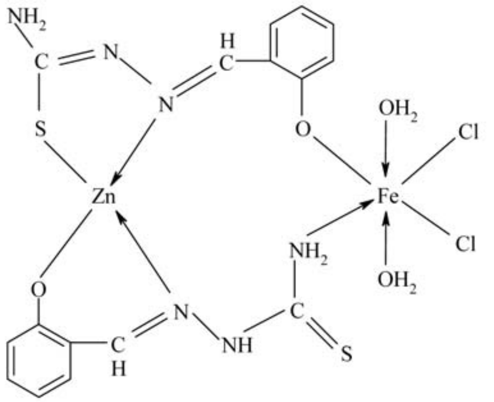

Figure 6. The proposed structure of the Fe(III) complex **(6)**.

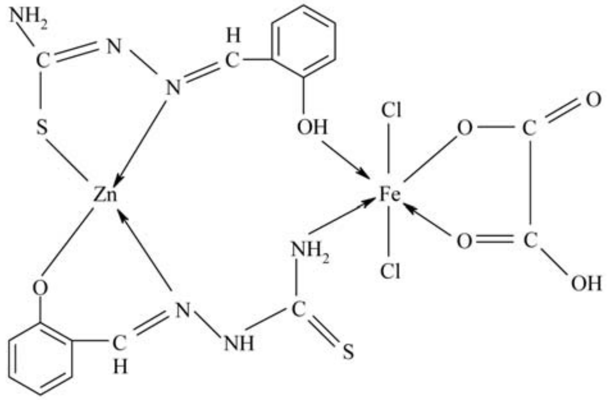

Figure 7. The proposed structure of the mixed-oxalato Fe(III) complex **(7)**.

3. 2. 3. 4. The Co(II) Complex

The reaction of $CoCl_2 \cdot 6H_2O$ with the complex ligand yielded the heterobinuclear complex (**8**), (Figure 5). The electronic spectrum of the obtained complex showed a band at 520 nm corresponding to $^4T_{1g}(F) \rightarrow {}^4A_{2g}(F)$ transition which is consistent with the octahedral geometry of the complex.[47] The effective magnetic moment of the complex is 5.0 B.M. which falls in the 4.7–5.2 B.M. range expected for octahedral cobalt(II) complexes.[48]

3. 2. 3. 5. The Ni(II) Complex

The reaction of $NiCl_2{\cdot}6H_2O$ with the complex ligand yielded the heterobinuclear complex (**9**) (Figure 5). Based on the electronic spectral and magnetic data, the nickel(II) complex, has the square-planar geometry with its characteristic features. The complex is diamagnetic, indicating a square planar geometry of the Ni(II) ion. The electronic spectrum of the complex (Table 3) showed two bands at 565 and 500 nm, corresponding to the $^1A_{1g} \rightarrow {}^1A_{2g}$ transition, confirming the square-planar geometry around the Ni(II) ion.[49] The ^1H and ^{13}C NMR spectral data of the complex (Table 4) lend further support of its suggested structure.

3. 2. 3. 6. The Cu(II) Complex

The Cu(II) complex, $[Zn(Tsc)_2CuCl(H_2O)]$, (Figure 8), was obtained from the reaction of the complex ligand with $CuCl_2 \cdot 2H_2O$. The electronic spectrum of the complex showed two absorption bands at 580 and 490 nm which may be corresponding to $^2B_{1g} \rightarrow {}^4A_{1g}$ and $^2B_{1g} \rightarrow {}^2E_g$, respectively, indicating the square planar geometry of the complex. The effective magnetic moment of the complex is 1.68 B.M. which is consistent with the proposed square planar structure.[50,51]

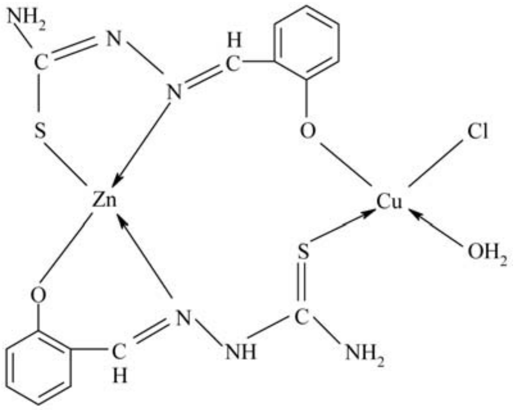

Figure 8. The proposed structure of the Cu(II) complex **(10)**.

3. 2. 3. 7. The Zn(II) Complex

The mononuclear Zn(II) complex, $[Zn(Tsc)(H_2O)]$, was obtained from the reaction of the complex ligand with $ZnCl_2$. The electronic spectrum of the complex exhibited one absorption band at 440 nm which is attributed to charge transfer transitions. The IR spectrum of the complex showed that the bands due to ν(C=N) and ν(C=S) were shifted to lower wave number. The new band observed at 1623 cm^{-1} may be due to the new azomethine group formed upon the loss of the NH proton. The ^1H NMR spectrum of the complex showed the disappearance of the phenolic OH and NH protons. ^{13}C NMR spectrum of the complex showed signals at 174.3, 164.1 and 152.6 ppm that may be assigned to C=S, C–O, and C=N groups, respectively. Based on the above interpretation, a tentative structure of the complex is shown in Figure 9.

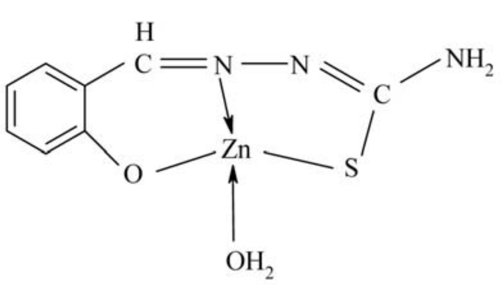

Figure 9. The proposed structure of the Zn(II) complex **(11)**.

3. 3. Antimicrobial Studies

The antimicrobial activity of the H_2L ligand, complex ligand and its heterobinuclear complexes was investigated against the sensitive organisms *Staphylococcus aureus* as Gram–positive bacteria, *Escherichia coli* as Gram–negative bacteria and the fungi *Candida albicans* and *Aspergillus flavus*. The results are listed in Table 5. Inspection of these data reveals that some of the tested compounds are biologically active against *Staphylococcus aureus* and *Escherichia coli*. Also, the complex ligand, $[Zn(Tsc)_2] \cdot H_2O$, $[Zn(Tsc)_2VO(SO_4)(H_2O)]$ and $[Zn(Tsc)_2CuCl(H_2O)]$ showed higher antifungal activity than its corresponding organic ligand and Amphotricine B as a control antifungal agent.

4. Conclusions

A complex ligand, $[Zn(Tsc)_2] \cdot H_2O$, was synthesized by the reaction of zinc acetate dihydrate with salicylaldehyde followed by the condensation with thiosemicarbazide. The reactions of the complex ligand with vanadyl(IV), manganese(II), iron(III), cobalt(II), nickel(II) and copper(II) gave a series of heterobinuclear complexes. On the other hand, the reaction of the complex ligand with zinc(II) ion gave a mononuclear complex. Characterization and structure elucidation of the complex ligand and the prepared complexes were achieved by elemental analyses, IR, electronic, mass, ^1H and ^{13}C NMR spectra as well as molar conductivity and magnetic measurements. The spectroscopic data showed that the complex ligand acts as a neutral bidentate with vanadyl(IV), manganese(II), iron(III) (in the presence of oxalic acid), cobalt(II) and nickel(II) ions. With copper(II) and iron(III) ions, it acts as a monobasic bidentate ligand. The prepared compounds showed antibacterial activity against the sensitive organisms *Staphylococcus aureus* as Gram–positive bacteria and *Escherichia coli* as Gram–negative bacteria and antifungal activity against the fungi *Candida albicans* and *Aspergillus flavus*.

5. References

1. D. X. West, J. K. Swearingen, J. Valdes-Martinez, S. Hernandez-Ortega, A.K. El-Sawaf, F. van Meurs, A. Castineiras, I. Garcia, E. Bermejo, *Polyhedron* **1999**, 18, 2919–2929.
2. P. Tarasconi, S. Capacchi, G. Pelosi, M. Cornia, R. Albertini, A. Bonati, P. Dall'Aglio, P. Lunghi, S. Pinelli, *Bioorg. Med. Chem.* **2000**, 8, 157–162.
3. S. E. Ghazy, M. A. Kabil, A. A. El-Asmy, Y.A. Sherief, *Anal. Lett.* **1996**, 29, 1215–1229.
4. J. R. Dilworth, A. H. Cowley, P. S. Donnelly, A. D. Gee, J. M. Heslop, *J. Chem. Soc. Dalton Trans.* **2004**, 2404–2412.
5. O. Mikhailov, M. Kazymova, T. Shumilora, S. Solovieva, *Trans. Met. Chem.* **2003**, 28, 665–667.
6. A. A. Abou-Hussen, N. M. El-Metwally, E. M. Saad, A. A. El-Asmy, *J. Coord. Chem.* **2005**, 58, 1735–1749.
7. T. S. Lobana, R. Sharma, G. Bawa, S. Khanna, *Coord. Chem. Rev.* **2009**, 253, 977–1055.
8. I. C. Mendes, F. B. Costa, G. M. de Lima, J. D. Ardisson, I. Garcia-Santos, A. Castiñeiras, H. Beraldo, *Polyhedron* **2009**, 28, 1179–1185.
9. J. Rivadeneira, D. A. Barrio, G. Arrambide, D. Gambino, L. Bruzzone, S. B. Etcheverry, *J. Inorg. Biochem.* **2009**, 103, 633–642.
10. D. Kovala-Demertzi, A. Papageorgiou, L. Papathanasis, A. Alexandratos, P. Dalezis, J. R. Miller, M. A. Demertzis, *Eur. J. Med. Chem.* **2009**, 44, 1296–1302.
11. P. I. S. Maia, F. R. Pavan, C. Q. F. Leite, S. S. Lemos, G. F. de Sousa, A. A. Batista, O. R. Nascimento, J. Ellena, E. E. Castellano, E. Niquet, V. M. Deflon, *Polyhedron* **2009**, 28, 398–406.

Table 5. Antimicrobial activity of the complex ligand and its complexes

Sample	**Mean* of zone diameter, nearest whole mm.** *Escherichia coli*	*Staphylococcus aureus*	*Candida albicans*	*Aspergillus flavus*
Control DMSO	0.0	0.0	0.0	0.0
Tetracycline (antibacterial agent)	32	34	–	–
Amphotricine B (antifungal agent)	–	–	21	17
H_2L (**1**)	13	14	12	13
$[Zn(Tsc)OAc] \cdot ½H_2O$ (**2**)	15	15	11	0.0
$[Zn(Tsc)_2] \cdot H_2O$ (**3**)	24	26	24	0.0
$[Zn(Tsc)_2VO(SO_4)(H_2O)]$ (**4**)	18	19	18	13
$[Zn(Tsc)_2MnCl_2(H_2O)_2]$ (**5**)	15	13	11	0.0
$[Zn(Tsc)_2FeCl_2(H_2O)_2]$ (**6**)	14	17	0.0	0.0
$[Zn(Tsc)_2Fe(ox)Cl_2]$ (**7**)	13	18	0.0	11
$[Zn(Tsc)_2CoCl_2(H_2O)_2]$ (**8**)	14	12	11	0.0
$[Zn(Tsc)_2NiCl_2]$ (**9**)	14	14	0.0	0.0
$[Zn(Tsc)_2CuCl(H_2O)]$ (**10**)	23	25	22	0.0
$[Zn(Tsc)(H_2O)]$ (**11**)	13	13	13	0.0

* Calculated from 3 values.

12. M. Belicchi-Ferrari, F. Bisceglie, A. Buschini, S. Franzoni, G. Pelosi, S. Pinelli, P. Tarasconi, M. Tavone, *J. Inorg. Biochem.* **2010**, 104, 199–206.
13. V. Vrdoljak, I. Đilović, M. Rubčić, S. K. Pavelić, M. Kralj, D. Matković–Čalogović, I. Piantanida, P. Novak, A. Rožman, M. Cindrić, *Eur. J. Med. Chem.* **2010**, 45, 38–48.
14. U. El-Ayaan, M. M. Youssef, S. Al-Shihry, *J. Mol. Stru.* **2009**, 936, 213–219.
15. M. S. Refat, I. M. El-Deen, Z. M. Anwer, S. El-Ghol, *J. Coord. Chem.* **2009**, 62, 1709–1718.
16. A. A. El-Asmy, O. A. Al-Gammal, D. A. Saad, S. E. Ghazy, *J. Mol. Stru.* **2009**, 934, 9–22.
17. M. Li, J. Zhou, H. Zhao, C. Chen, J. Wang, *J. Coord. Chem.* **2009**, 62, 1423–1429.
18. C. Marzano, M. Pellei, F. Tisato, C. Santini, *Anticancer Agents Med. Chem.* **2009**, 9, 185–211.
19. R. Kruszynski, B. Machura, M. Wolff, J. Kusz, J. Mroziñski, A. Bieñko. *Inorg. Chim. Acta* **2009**, 362, 1369–1373.
20. O. Kahn, *Adv. Inorg. Chem.* **1995**, 43, 179–259.
21. K. S. Murray, *Adv. Inorg. Chem.* **1995**, 43, 261–358.
22. W. R. Browne, R. Hage, J. G. Vos, *Coord. Chem. Rev.* **2006**, 250, 1653–1668.
23. V. Rajendiran, R. Karthik, M. Palaniandavar, H. Stoeckli-Evans, V. Subbarayan Periasamy, M. A. Akbarsha, B. S. Srinag, H. Krishnamurthy, *Inorg. Chem.* **2007**, 46, 8208–8221.
24. M. Trivedi, D. S. Pandey, N. P. Rath, *Inorg. Chim. Acta* **2009**, 362, 284–290.
25. T. Rüffer, B. Bräuer, F. E. Meva, L. Sorace, *Inorg. Chim. Acta* **2009**, 362, 563–569.
26. A. W. Bauer, W. W. M. Kirby, J. C. Sherris, M. Turck, *Am. J. Clin. Pathol.* **1966,** 45, 493–496.
27. D. C. Gross, S. E. De Vay, *Physiol. Plant Pathol.* **1977**, 11, 13–28.
28. M. Shebl, H. S. Seleem, B. A. El-Shetary, *Spectrochim. Acta, Part A* **2010**, 75, 428–436.
29. H. S. Seleem, B. A. El-Shetary, S. M. E. Khalil, M. Mostafa, M. Shebl, *J. Coord. Chem.* **2005**, 58, 479–493.
30. J. Vančo, J. Marek, Z. Trávníček, E. Račanská, J. Muselík, O. Švajlenová, *J. Inorg. Biochem.* **2008**, 102, 595–605.
31. D. K. Sau, R. J. Butcher, S. Chaudhuri, N. Saha, *Polyhedron* **2004**, 23, 5–14.
32. M. Shebl, *Spectrochim. Acta, Part A* **2009**, *73,* 313–323.
33. S. Sen, S. Shit, S. Mitra, S. R. Batten, *Struct. Chem.* **2008**, 19, 137–142.
34. İ. Demir, M. Bayrakci, K. Mutlu, A. İ. Pekacar, *Acta Chim. Slov*. **2008**, 55, 120–124.
35. H. Beraldo, W. F. Nacif, L. R. Teixeira, J. S. R. Rebouças, *Trans. Met. Chem.* **2002**, 27, 85–88.
36. U. B. Gangadharmath, V. K. Revankar, V. B. Mahale, *Spectrochim. Acta, Part A* **2002**, 58, 2651–2657.
37. M. Shebl, *Spectrochim. Acta, Part A* **2008**, 70, 850–859.
38. N. M. El-Metwally, R. M. El-Shazly, I. M. Gabr, A. A. El-Asmy, *Spectrochim. Acta, Part A* **2005**, 61, 1113–1119.
39. P. S. Subramanian, P. C. Dave, V. P. Boricha, D. Srinivas, *Polyhedron* **1998**, 17, 443–448.
40. M. El-Behery, H. El-Twigry, *Spectrochim. Acta, Part A* **2007**, 66, 28–36.
41. F. A. Walker, R. L. Carlin, R. H. Rieger, *J. Chem. Phys.* **1966**, 45, 4181–4189.
42. A. A. A. Abou-Hussen, A. A. A. Emara, *J. Coord. Chem.* **2004**, 57, 973–987.
43. S. Chandra, A. Kumar, *Spectrochim. Acta, Part A* **2007**, 68, 469–473.
44. S. M. E. Khalil, *J. Coord. Chem.* **2003**, 56, 1013–1024.
45. J. C. Bailar, H. J. Emeleus, R. Nyholm, A. F. Trotman-Dickenson, *Comprehensive Inorganic Chemistry*, Pergamon Press, New York, **1975**, pp.1153, 1089, 1048 and 517.
46. M. Shebl, *J. Coord. Chem.* **2009**, 62, 3217–3231.
47. E. Viñuelas-Zahínos, M. A. Maldonado-Rogado, F. Luna-Giles, F. J. Barros-García, *Polyhedron* **2008**, 27, 879–886.
48. K. A. R. Salib, S. L. Stefan, S. M. Abu El-Wafa, H. F. El-Shafiy, *Synth. React. Inorg. Met.-Org. Chem.* **2001**, 31, 895–915.
49. K. R. Krishnapriya, M. Kandaswamy, *Polyhedron* **2005**, 24, 113–120.
50. S. M. E. Khalil, H. S. Seleem, B. A. El-Shetary, M. Shebl, *J. Coord. Chem.* **2002**, 55, 883–899.
51. H. S. Seleem, B. A. El-Shetary, M. Shebl, *Heteroatom. Chem.* **2007**, 18, 100–107.

Povzetek

Z uporabo mononuklearnega kompleksa $[Zn(Tsc)_2] \cdot H_2O$ kot kompleksnega liganda za vanadilove(IV), manganove(II), železove(III), kobaltove(II), nikljeve(II) in bakrove(II) ione, smo sintetizirali heterobinuklearne komplekse. Kompleksni ligand smo pripravili z reakcijo med cinkovim acetatom dihidratom, ki ji je sledila kondenzacija s tiosemikarbazidom. Strukturo kompleksnega liganda in heterobinuklearnih koordinacijskih spojin smo določili z elementno analizo, IR, elektronsko, masno, ^1H and ^{13}C NMR spektroskopijo kot tudi z merjenjem molske prevodnosti in magnetne susceptibilnosti. Kompleksi s formulami $[Zn(Tsc)_2VO(SO_4)(H_2O)]$, $[Zn(Tsc)_2MCl_2(H_2O)_2]$ (M = Mn, Fe in Co), $[Zn(Tsc)_2Fe(ox)Cl_2]$ in $[Zn(Tsc)_2NiCl_2]$ imajo oktaedrično geometrijo, medtem ko je kompleks $[Zn(Tsc)_2CuCl(H_2O)]$ kvadratno-planaren. Kompleksni ligand in njegovi heterobinuklearni kompleksi kažejo antibakterijsko aktivnost proti Gram-pozitivni bakteriji *Staphylococcus aureus* in Gram–negativni bakteriji *Escherichia coli* in aktivnost proti glivam *Candida albicans* and *Aspergillus flavus*.